Stress intensity factors for an interface crack between an epoxy and aluminium composite plate

S. Itou[†]

*Department of Mechanical Engineering, Kanagawa University, Rokkakubashi,
Kanagawa-ku, Yokohama 221-8686, Japan*

Abstract. A cracked composite specimen, comprised of an epoxy and an aluminium plate, was fractured under a tensile load. In this paper, two crack configurations were investigated. The first was an artificial center crack positioned in the epoxy plate parallel to the material interface. The other was for two edge cracks in the epoxy plate, again, parallel to the interface. A tensile test was carried out by gradually increasing the applied load and it was verified that the cracks always moved suddenly in an outward direction from the interface. The d/a ratio was gradually reduced to zero, and it was confirmed that the maximum stress intensity factor value for the artificial center crack, $K_{\theta\theta}^{max}$, approached that of an artificial interface crack, $K_{\theta\theta}^{ifc\ max}$ (where: $2a$ is the crack length and d is the offset between the crack and interface). The same phenomenon was also verified for the edge cracks. Specifically, when the offset, d, was reduced to zero, the maximum stress intensity factor value, $K_{\theta\theta}^{max}$, approached that of an artificial interface edge crack.

Keywords: stress intensity factor; parallel crack; interface crack; epoxy-aluminium composites; tensile test.

1. Introduction

Three kinds of solutions are typically provided for an interface crack located at the interface between composite materials. The first is an exact solution given by England (1965). However, this solution does not satisfy the physical conditions. Specifically, the solution contains oscillatory stress singularities and interpenetration of the materials around the crack tip. In reality, interpenetration does not occur at crack tips in composite materials. Because of this, Comninou (1977) presented the second solution. This includes a contacting area around the crack end. However, the present author believes that a weakness exists in this solution. More specifically, when the material properties of the two dissimilar half-planes approach each other, the solution approaches that of a crack in a homogeneous elastic material. However, the Mode I stress intensity factor, K_1, cannot be determined if the contact solution is used. Interfaces are usually very rough and interdigitated. Considering this, in the third solution Mak *et al.* (1980) introduced a no-slip zone near the crack tips prohibiting relative shearing motions. The stress singularities in these three solutions differ markedly. Consequently, the best choice of solution is difficult as a judgment must be made on whether the

---

† Ph.D., E-mail: itous001@kanagawa-u.ac.jp

crack is presently harmless or unstable and dangerous with the possibility of rapid breakdown.

The irregular behavior, appearing in both the exact and contact solutions, is restricted to only a very small area around the crack tip. The stresses outside this region are similar to those present near a crack in a homogeneous material. Considering this fact, the opening model for an interface crack presented herein assumes that the stress singularities are similar to those of an ordinary crack in a homogeneous material (Zhou *et al.* 2004, Zhou and Wang 2004, Sun *et al.* 2004, Zhou *et al.* 2004, 2005). Another approach to obtaining a physically acceptable solution is to consider the case of an interface crack in the non-homogeneous thin layer between the dissimilar elastic materials (Delale and Erdogan 1988, Ozturk and Erdogan 1996, Snbeeb and Binienda 1999, Li *et al.* 2002, Chen 2005).

If a crack exists within one of two dissimilar bonded half-planes instead of at the interface, it is possible, and acceptable from a physical viewpoint, that the stresses have normal singularities. Consider a crack of length $2a$ in an epoxy half-plane bonded to an aluminium half-plane with the crack parallel to, but offset from the interface by the distance, d. Now, assume the stress intensity factors for an interface crack are defined as those for a crack in a homogeneous plate (the definition of $K_{\theta\theta}^{\max}$ is shown in detail in Eq. (2)). If it is shown experimentally that the $K_{\theta\theta}^{\max}$ value for a crack in the epoxy half-plane agrees well with the $K_{\theta\theta}^{ifc\ \max}$ value for an interface crack as the d/a ratio approaches zero, this would verify that the stress intensity factor for an artificial interface crack can be defined in the same manner as for a conventional crack.

The author has previously assumed that the stress intensity factor for an artificial interface crack can be defined in the same way as a crack in a non-homogeneous plate. Experiments were conducted to obtain the maximum stress intensity factor, $K_{\theta\theta}^{ifc\ \max}$, for epoxy-aluminium composite plates weakened by an artificial interface crack (Itou 2004). The experimental results thereof for an artificial interface crack, $K_{\theta\theta}^{ifc\ \max}$, agree well with the theoretical result of a crack in an epoxy plate, $K_{\theta\theta}^{\max}$, when d/a is very small. However, those experiments were only performed for an interface crack.

It is worthwhile confirming whether or not the maximum stress intensity factor for a crack in an epoxy plate, $K_{\theta\theta}^{\max}$, approaches that for an interface crack, $K_{\theta\theta}^{ifc\ \max}$, when the d/a ratio is reduced to zero. In this paper, experiments were carried out for an artificial center crack in an epoxy plate. These experiments verify that the value for an artificial interface crack, $K_{\theta\theta}^{ifc\ \max}$, is very close to that of a crack in the epoxy plate near the interface, $K_{\theta\theta}^{\max}$. As a result, it can be concluded that the maximum stress intensity factor for an artificial interface crack, $K_{\theta\theta}^{ifc\ \max}$, which is a physically acceptable solution, can be obtained by calculating the stress intensity factor for a parallel crack placed near the interface of, and in the softer of, two composite plates. This phenomenon was also verified through similar experiments conducted for two edge cracks in the epoxy part of a composite epoxy-aluminium plate.

2. Experiments

2.1 Experiments for an artificial center crack

2.1.1 Test specimen

As in the previously mentioned study by the author (Itou 2004), an artificially cracked epoxy-aluminium composite specimen was made. In order to accurately position the crack in the epoxy
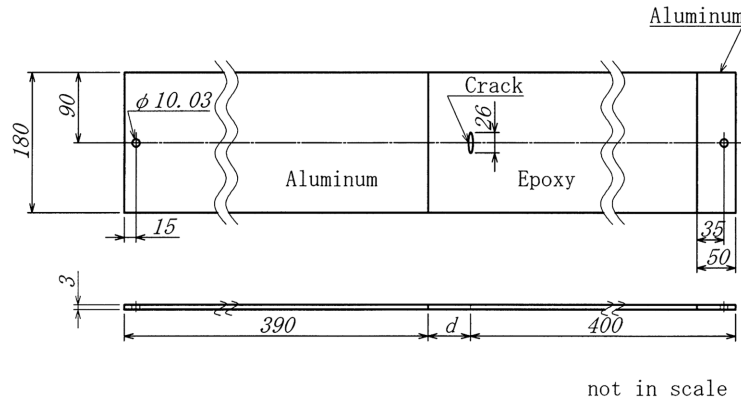
Fig. 1 Configuration of test specimen for a central crack

plate, the epoxy resin casting was produced in two steps. First, a 3 mm thick epoxy plate, detailed in Fig. 1 of the author's previous paper (Itou 2004), was made. Next, a mold was constructed using this epoxy plate and a 3 mm thick aluminium plate, as shown in Fig. 9 of the same paper. In this step some 0.07 mm thick Teflon tape was affixed to the edge of the epoxy plate. Finally, epoxy resin was cast into the mould to generate the test specimen, as shown in Fig. 1. The width, $2h$, crack length, $2a$, and thickness, t, were 180 mm, 26 mm, and 3 mm respectively.

2.1.2 Fracture of the test specimens

A tensile load was applied to the test specimen with a tensile tester and slowly increased. When the tensile load reached a maximum value, P_f, the specimen fractured suddenly and without warning. As examples, the fracture patterns shown in Fig. 2 are for $d/a = 0.0$, 1.272, and 5.772. For clarity, the interface, the crack and the crack path are highlighted with blue, purple and red lines respectively. As can be seen from the figure, the cracks always depart from the interface and propagate further into the epoxy half of the composite plate. Two polar coordinate systems, (r_R, θ_R) and (r_L, θ_L), are employed for the epoxy plate to more clearly express the initial departure angle of

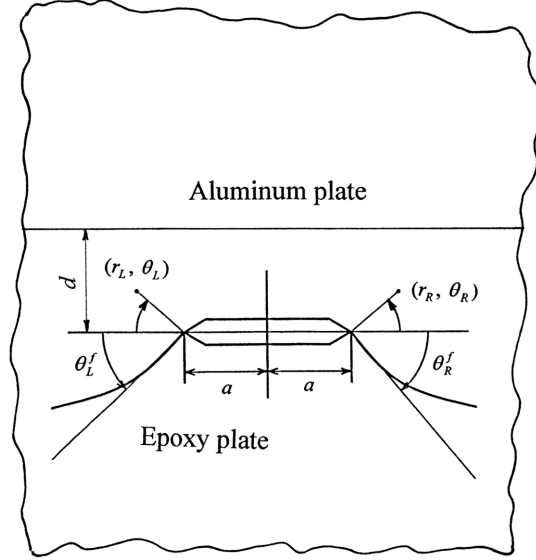Fig. 2 Fracture patterns ($d/a = 0.0$, 1.272, 5.772)

Fig. 3 Two polar coordinate systems and the initial crack angles

the crack. These coordinate systems are shown in Fig. 3. The initial departure angles of the cracks are denoted by the following equation

$$\theta_R = \theta_R^f, \qquad \theta_L = \theta_L^f \tag{1}$$

Experiments were conducted for several offsets, d. The values of $d, 2a, 2h, t, P_f, \theta_R^f$ and θ_L^f were measured and recorded for each experiment.

2.1.3 Stress intensity factors

Erdogan and Sih (1963) conducted experiments in which they confirmed that a crack in a brittle material moves along the plane of maximum tensile stress. If the coordinate system (r_R, θ_R) in Fig. 3 is replaced by (r, θ), and the maximum tensile stress around the crack tip is denoted by $\tau_{\theta\theta}^{max}$, the stress intensity factor, $K_{\theta\theta}^{max}$, is defined by the equation

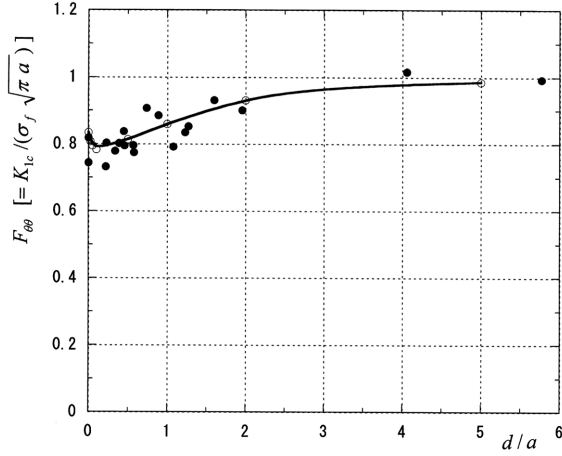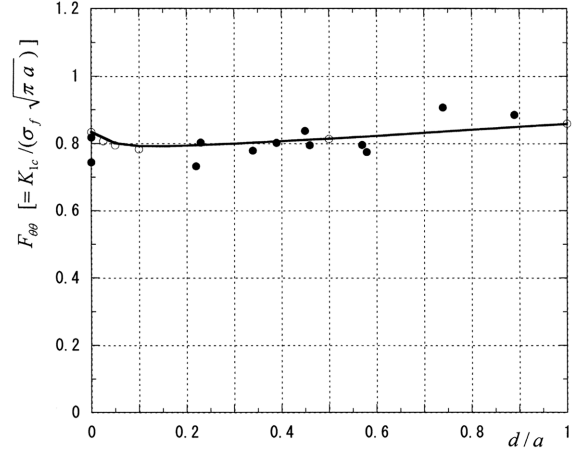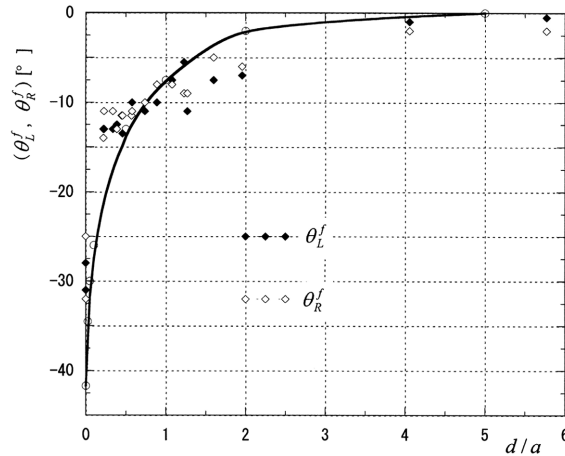$$K_{\theta\theta}^{max} = \lim_{r \to 0} \sqrt{2\pi r} \quad \tau_{\theta\theta}^{max} = \sigma\sqrt{\pi a}\, F_{\theta\theta}(d/a) \tag{2}$$

If the specimen breaks as the tensile stress, σ, reaches σ_f, the maximum stress intensity factor can be assumed to have reached the fracture toughness value of the epoxy resin plate, K_{1c}. Thus, $F_{\theta\theta}(d/a)$ can be obtained by the following equation

$$F_{\theta\theta}(d/a) = K_{1c}/(\sigma_f\sqrt{\pi a}) \tag{3}$$

The fracture toughness value for an artificial crack in epoxy resin, K_{1c}, for a plate with a center crack has previously been experimentally determined by the author (Itou 2004) as

$$K_{1c} = 1.147 \times 10^6 \text{ N/m}^{1.5} \tag{4}$$

Fig. 4 Stress intensity factor for $0 \leq d/a < 6.0$

Fig. 5 Stress intensity factor for $0 \leq d/a < 1.0$

Fig. 6 Initial crack angles for $0 \leq d/a < 6.0$

Using this result, the values of $F_{\theta\theta}(d/a)$ were calculated for $0 \leq d/a < 6.0$ and are shown in Fig. 4. One of the purposes of this study is to determine whether or not the value of $F_{\theta\theta}(d/a)$ reaches that of an artificial interface crack, $F_{\theta\theta}^{ifc}(d/a)$, as d/a approaches zero. Thus, the results are shown in more detail for $0 \leq d/a < 1.0$ in Fig. 5. The experimental data for the initial crack departure angles, θ_R^f and θ_L^f, are shown in Fig. 6. In Figs. 4, 5 and 6, the values at $d/a = 0$ are equivalent to those for an interface crack.

In this study, the a/h ratio was fixed at 0.1444 so as to reduce the affect of the specimen's stress free edges on the stresses around the crack tips. Consider two dissimilar elastic half-planes with a crack parallel to the interface, as shown in Fig. 7. A Cartesian coordinate system (x, y) and polar coordinate system (r, θ) are also displayed in this figure. The stresses for an epoxy-aluminium composite subject to a tensile load were determined by the author in the previously mentioned study (Itou 2004). Moreover, numerical calculations were carried out for the case of a crack in the epoxy half-plane. These calculations used material properties for aluminium of $E = 70.5$ GPa and $v = 0.35$,
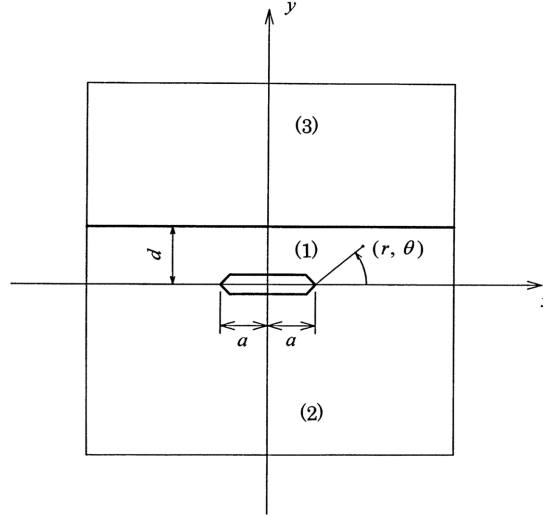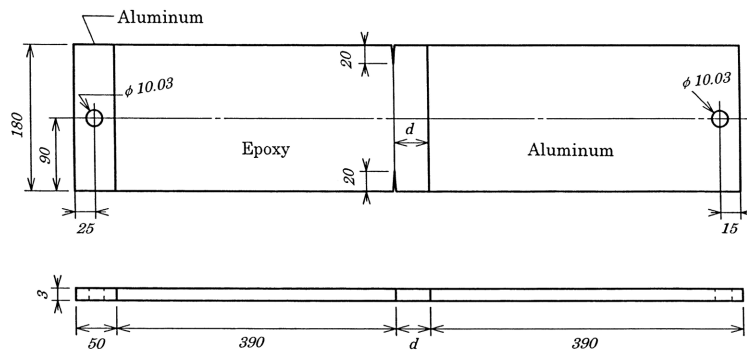
Fig. 7 Crack in a half-plane bonded to a dissimilar half-plane

and material properties for epoxy of $E = 5.6$ GPa and $v = 0.34$. The numerical results for the maximum stress intensity factor, $K_{\theta\theta}^{\max}$, are depicted by the solid lines in Figs. 4 and 5. The angles at which the maximum stress intensity factor, $K_{\theta\theta}^{\max}$, occurs are also shown by the solid line in Fig. 6. It should be noted that the experimental $K_{\theta\theta}^{ifc\ \max}$ result for $d/a = 0.0$ was obtained from an artificial interface crack fabricated by placing Teflon tape directly onto the edge of the aluminium plate when the mold was made. The theoretical values for $d/a = 0.0$ cannot be calculated. Therefore, the numerical results at $d/a = 0.0$ in Figs. 4, 5 and 6 are not those for $d/a = 0.0$, but those for $d/a \rightarrow 0.0$. The process employed to calculate the values for $d/a \rightarrow 0.0$ is described in detail by the author in the previously mentioned study (Itou 2004).

The experimentally obtained values of maximum stress intensity factor, $K_{\theta\theta}^{\max}$, clearly agree well with the corresponding theoretically calculated values, similarly for the initial crack departure angle. This is strong validation for the experimental method employed in this study.

not in scale

Fig. 8 Configuration of test specimen for two symmetric edge cracks

2.2 Experiments for two artificial edge cracks

2.2.1 Test specimen

An epoxy-aluminium composite specimen was made using a method similar to that described in Section 2.1. Two edge cracks of equal length, *a*, were placed in the epoxy plate, as shown in Fig. 8. The width, 2*h*, crack length, *a*, and thickness, *t*, of the plate were 180 mm, 20 mm, and 3 mm respectively. It should be noted that the crack length is denoted by the symbol, *a*.

2.2.2 Fracture of the test specimens

Two polar coordinate systems, (r_R, θ_R) and (r_L, θ_L), are employed on the epoxy plate in order to express the initial crack departure angle, as shown in Fig. 9. The initial crack departure angles are denoted as follows

$$\theta_R = \theta_R^f, \qquad \theta_L = \theta_L^f \tag{5}$$

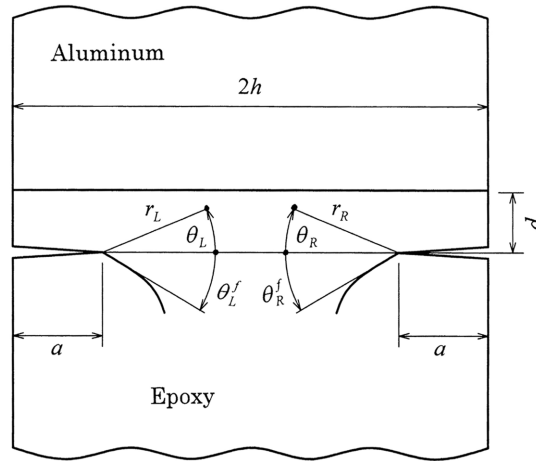Fig. 9 Two polar coordinate systems and the initial crack angles

Fig. 10 Fracture patterns (*d/a* = 0.0, 1.0, 5.55)

Experiments were carried out for several offsets, *d*. Typical fracture patterns for *d/a* = 0.0, 1.0 and 5.55 are shown in Fig. 10. It was assumed that the cracks started at the tip of the arrows in the figure. This is because the fractured area is typically larger in the crack extension area. For edge cracks, it was observed that the fracture always starts from one end of a crack and that both cracks do not propagate simultaneously. The values of *d*, *a*, *2h*, *t*, P_f, θ_R^f, and θ_L^f were measured and recorded for each experiment.

2.2.3 Stress intensity factors

The stress intensity factor, $K_{\theta\theta}^{max}$, can be determined for the edge cracks using a procedure similar to that employed in Section 2.1 and given by the following equation

$$K_{\theta\theta}^{max} = \lim_{r \to 0} \sqrt{2\pi r} \quad \tau_{\theta\theta}^{max} = \sigma\sqrt{\pi a}\, F_{\theta\theta}(d/a) \qquad (6)$$

Form this, the dimensionless stress intensity factor, $F_{\theta\theta}(d/a)$, can be expressed by the equation

$$F_{\theta\theta}(d/a) = K_{1c}/(\sigma_f\sqrt{\pi a}) \qquad (7)$$

The values of $F_{\theta\theta}(d/a)$ for $0 \le d/a < 15.0$, calculated using the experimental data, are shown in Fig. 11. The experimental data for the initial crack departure angles, θ_R^f or θ_L^f, are detailed in Fig. 12. Note that, in Figs. 11 and 12, the values at *d/a* = 0 are those for the interface crack. In Figs. 4, 5 and 6 of Section 2.1, the solid lines depict the theoretical results. However, the solid lines in Figs. 11 and 12, represent curves fitted to the experimental results and not the theoretical results.

The $F_{\theta\theta}(d/a)$ value for $d/a \to \infty$ is given by the equation (Tada 2000)

$$F_{\theta\theta}(d/a) = [1.122 - 0.561 \times (a/h) - 0.206 \times (a/h)^2 + 0.471 \times (a/h)^3 - 0.190 \times (a/h)^4]$$
$$/\sqrt{(1-a/h)} \qquad (8)$$

The dotted straight line in Fig. 11 represents the value calculated from Eq. (8). As the *d/a* ratio increases, the experimental results for $F_{\theta\theta}(d/a)$ must approach the value calculated from Eq. (8).
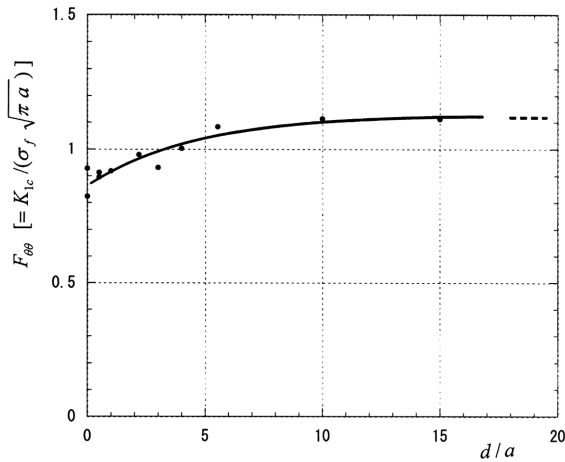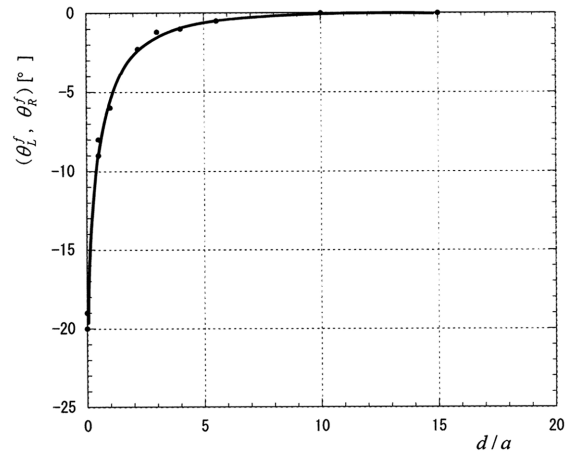

Fig. 11 Stress intensity factor for $0 \le d/a < 15.0$ Fig. 12 Initial crack angles for $0 \le d/a < 15.0$

Also, the initial crack departure angles, θ_R^f and θ_L^f, must approach zero. Figs. 11 and 12 verify these facts. This is further validation for the experimental method employed in this study.

The maximum value of the stress intensity factor $K_{\theta\theta}^{\max}$ clearly approaches the value of $K_{\theta\theta}^{ifc\ \max}$ as d/a approaches zero. The same applies for the initial crack departure angle.

3. Discussion

3.1 Energy release rate in the exact solution

Consider an interface crack between the upper half-plane (1) and the lower half-plate (2), as shown in Fig. 13, where the crack is located along the x-axis from $-a$ to $+a$ at $y = 0$ in the Cartesian coordinate system (x, y). The corresponding polar coordinates (r, θ) can be calculated using the equation

$$x = a + r\cos(\theta), \qquad y = r\sin(\theta) \tag{9}$$

Let us consider that the right-hand side of the crack end moves slightly along the x-axis from $x = a$ to $x = a + \Delta a$ at $y = 0$, as shown in Fig. 14. In this case, the energy release rate g is expressed by the definition

$$g = \lim_{\Delta a \to 0} \frac{1}{\Delta a \times t \times 2} \int_0^{\Delta a} \{ \tau_{yy1}(a+r) \times t[v_1(a+r) - v_2(a+r)]$$
$$+ \tau_{xy1}(a+r) \times t[u_1(a+r) - u_2(a+r)] \} \, dr \tag{10}$$

where t is the thickness of the plate, τ_{yy}, τ_{xy} are stresses, and u, v are the x and y components of the displacement, respectively. Subscripts 1 and 2 indicate half-planes (1) and (2), respectively. When the crack end separates and advances a very small distance Δa, the crack end definitely moves
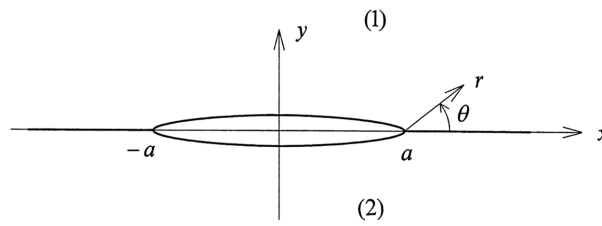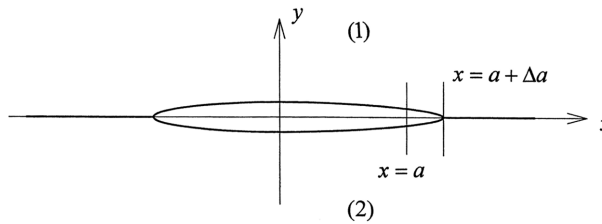

Fig. 13 An interface crack

Fig. 14 Crack extension length Δa

along the x-axis, not along the interpenetrating shapes of the displacements u and v given in the exact solution. If the stresses and displacements in the exact solutions are submitted in Eq. (10), the oscillatory property disappears in the energy release rate g. However, it is very difficult for the present author to accept that the energy release rate g defined in the exact solution is useful in fracture mechanics.

3.2 Experimental results for artificial interface cracks

Two kinds of epoxy-aluminium composite plate test pieces were made in order to confirm whether or not the maximum value of the stress intensity factor, $K_{\theta\theta}^{\max}$, for a crack in the epoxy half approaches the $K_{\theta\theta}^{ifc\ \max}$ value for an artificial interface crack as the position of the crack is gradually moved closer to the interface. In one test, a central crack was located parallel to the interface, while two edge cracks are employed in another test. The artificial interface cracks were fabricated by placing Teflon tape directly onto the end of the aluminium plate when the mold was formed.

The results of both experiments indicate that the maximum value of the stress intensity factor, $K_{\theta\theta}^{\max}$, approaches that for an artificial interface crack, $K_{\theta\theta}^{ifc\ \max}$, as the crack position becomes closer to the interface. Figs. 4, 5 and 11 suggest that the stress intensity factors for an interface crack, which is defined in the conventional manner, can be approximated for dissimilar elastic materials by placing a parallel crack in the softer material close to the interface.

There question arises whether or not the interface crack always moves outward from the interface. In the authors' recent work (Itou *et al.* 2006), it has been shown that the artificial interface crack does indeed always move outward from the interface as long as the average roughness, R_a, of the surface of the edge of the aluminium is larger than 0.65 μm. If R_a is smaller than 0.60 μm, the artificial interface crack tends to extend along the interface. Consequently, the results presented in this paper only apply to cases where R_a for the surface of the edge of the aluminium is larger than 0.65 μm.

3.3 Crack extension along the interface

If the interface crack moves, not outward from, but along the interface, the fracture criterion may be somewhat different from that employed herein. For this case, it may be necessary to determine the fracture toughness value, K_{1c}^{if}, for an interface crack which extends along the interface. To obtain this value, the aluminium edge surface should be polished until the average roughness, R_a, is smaller than 0.60 μm. The value K_{1c}^{if} is probably determined by using the stress intensity factor for a crack which is placed in the epoxy plate near the interface, K_1^{near}. In this case, the composite material, weakened by an interface crack, fractures when the K_1^{near} value becomes larger than the K_{1c}^{if} value. However, this is only a hypothesis and should be verified experimentally.

It should be noted that the cracks were artificially formed in the epoxy plate using 0.07 mm thick Teflon tape. Further experiments should be conducted to determine if the thickness of the artificial crack affects the results.

References

Chen, J. (2005), "Determination of thermal stress intensity factors for an interface crack in a graded orthotropic

coating-substrate structure", *Int. J. Fracture.*, **133**, 303-328.

Comninou, M. (1977), "The interface crack", *J. Appl. Mech.*, ASME, **44**, 631-636.

Delale, F. and Erdogan, F. (1988), "Interface crack in a nonhomogeneous elastic medium", *Int. J. Eng. Sci.*, **28**, 559-568.

England, A.H. (1965), "A crack between dissimilar media", *J. Appl. Mech.*, ASME, **32**, 400-402.

Erdogan, F. and Sih, G.C. (1963), "On the crack extension in plates under plane loading and transverse shear", *J. Basic Eng.*, ASME, **85**, 519-527.

Itou, S. (2004), "An experiment on stress intensity factors for an interface crack between epoxy and aluminium plate", *Int. J. Fracture*, **125**, 89-102.

Itou, S., Hashimoto, Y. and Oikawa, T. (2006), "The effect of the surface roughness of the aluminium edge surface on the crack initial angle for an artificial interface crack between aluminium and epoxy composites (in Japanese)", *Report of Dept. Mech. Eng., Kanagawa University*, 25-26.

Li, C., Duan, Z. and Zou, Z. (2002), "Torsional impact response of a penny-shaped interface crack in bonded materials with a graded material interlayer", *J. Appl. Mech.*, ASME, **69**, 303-308.

Mak, A.F., Keer, L.M., Chen, S.H. and Lewis, J.L. (1980), "A no-slip interface crack", *J. Appl. Mech.*, ASME, **47**, 347-350.

Ozturk, M. and Erdogan, F. (1996), "Axisymmetric crack problem in bonded materials with a graded interfacial region", *Int. J. Solids Struct.*, **33**, 193-219.

Snbeeb, N.I. and Binienda, W.K. (1999), "Analysis of an interface crack for a functionally graded strip sandwiched between two homogeneous layers of finite thickness", *Eng. Fract. Mech.*, **64**, 693-720.

Sun, Y.G., Zhou, Z.G. and Wu, L.Z. (2004), "Investigating the behaviour of a Griffith crack at the interface between isotropic and orthotropic elastic half-planes for the opening crack mode", *JSME Int. J.* (Series A), **47**, 457-466.

Tada, H. (2000), *The Stress Analysis of Cracks Handbook*, The ASME, New York.

Zhou, Z.G., Wang, B. and Sun, Y.G. (2004), "Investigation of the behavior of a Griffith crack at the interface of a layer bonded to a half plane using the Schmidt method for the opening crack mode", *Mech. Res. Commun.*, **31**, 545-555.

Zhou, Z.G. and Wang, B. (2004), "Investigation of the behavior of a Griffith crack at the interface between two dissimilar orthotropic elastic half-planes for opening crack mode", *Appl. Math. Mech.*, **25**, 730-740.

Zhou, Z.G., Wang, B. and Yang, L.J. (2004), "Investigation of the behavior of an interface crack between two half-planes of orthotropic functionally graded materials by using a new method", *JSME Int. J.* (Series A), **47**, 467-478.

Zhou, Z.G., Wang, B. and Wu, L.Z. (2005), "Investigation of the behavior of a crack between two half-planes of functionally graded materials by using the Schmidt method", *Struct. Eng. Mech.*, **19**, 425-440.